Ozaki, N., Kanehira, S., Hayashi, Y., Ohkouchi, S., Ikeda, N., Sugimoto, Y. and Hogg, R. A. (2017) Growth of quantum three-dimensional structure of InGaAs emitting at ~1 µm applicable for a broadband near-infrared light source. Journal of Crystal Growth, 477, pp. 230-234.

There may be differences between this version and the published version. You are advised to consult the publisher's version if you wish to cite from it.

http://eprints.gla.ac.uk/151403/

Deposited on: 10 November 2017

Enlighten – Research publications by members of the University of Glasgow
http://eprints.gla.ac.uk

Growth of quantum three-dimensional structure of InGaAs emitting at ~1 μm applicable for a broadband near-infrared light source

Nobuhiko Ozaki[1,*], Shingo Kanehira[1], Yuma Hayashi[1], Shunsuke Ohkouchi[2], Naoki Ikeda[3], Yoshimasa Sugimoto[3], and Richard A. Hogg[4]

[1]*Faculty of Systems Engineering, Wakayama University, 930 Sakaedani, Wakayama, Wakayama 640-8510, Japan*

[2]*NEC Corporation, 34, Miyukigaoka, Tsukuba, Ibaraki 305-8501, Japan*

[3]*National Institute for Materials Science (NIMS), 1-2-1 Sengen, Tsukuba, Ibaraki 305-0047, Japan*

[4] *School of Engineering, University of Glasgow, Rankine Building, Glasgow, G12 8LT UK*

Abstract

We obtained a high-intensity and broadband emission centered at ~1 μm from InGaAs quantum three-dimensional (3D) structures grown on a GaAs substrate using molecular beam epitaxy. An InGaAs thin layer grown on GaAs with a thickness close to the critical layer thickness is normally affected by strain as a result of the lattice mismatch and introduced misfit dislocations. However, under certain growth conditions for the In concentration and growth temperature, the growth mode of the InGaAs layer can be transformed from two-dimensional to 3D growth. We found the optimal conditions to obtain a broadband emission from 3D structures with a high intensity and controlled center wavelength at ~1 μm. This method offers an alternative approach for fabricating a broadband near-infrared light source for telecommunication and medical imaging systems such as for optical coherence tomography.

Keywords: A3.Molecular beam epitaxy, B1.Nanomaterials, B2.Semiconducting III-V materials, B3. Infrared devices

*Corresponding author:
E-mail: ozaki@sys.wakayama-u.ac.jp

1. Introduction

Broadband near-infrared (NIR) light sources are widely used in various fields such as telecommunication and medical imaging. For instance, optical coherence tomography (OCT) [1], which is a non-invasive profile imaging system, requires a broadband light source for its probe. OCT operates based on low-coherent interference, where the bandwidth of the light source is inversely proportional to the axial resolution of the OCT image [2]. Thus, a broader light source contributes to a higher resolution. In addition, an emission centered close to 1 μm is preferable for obtaining a large imaging depth in aqueous tissues because of the low optical absorptions of hemoglobin and water in a biological sample [3]. To meet such requirements, we developed a broadband light source based on InAs quantum dots (QDs) grown on GaAs [4–10]. The self-assembled InAs QD ensemble has an inherent size distribution that produces a broadband emission [11]. Thus, it has been recognized as an ideal light emitting material for an OCT light source [12,13]. When InAs QDs are grown on GaAs, they normally emit a broadband spectrum centered at 1.2–1.3 μm. The center emission wavelength, however, should be controlled close to 1 μm. Although we attempted to blue-shift the QD emission wavelength using several methods [14,15], controlling the emission's center wavelength at ~1 μm while maintaining the emission intensity has been difficult.

On the other hand, it is easy to control the center wavelength of the emission of an InGaAs thin layer grown as a quantum well (QW) on GaAs at ~1 μm using an optimal thickness and In concentration while maintaining the emission intensity, although broadband emission is not available. In addition, the InGaAs/GaAs system is influenced by the strain due to the lattice mismatch between them, and the optimal conditions for the QW growth are limited. The QW thickness should be below a critical layer thickness (CLT) at a certain In concentration. Thus, it was recognized as an inconvenient material to realize a broadband emission near 1 μm. However, in the preliminary work for the InGaAs QW growth, it was

reported that a growth mode transformation from two-dimensional (2D) to three-dimensional (3D) growth occurred close to the CLT, and resulted in a broadband emission [16,17]. In the previous study, measurements was taken to avoid this 3D transformation because the purpose of the study was the investigation of the CLT for QW growth and the dependence of the CLT on the growth temperature. In this study, however, we focused on the 3D structure that appeared in the InGaAs/GaAs system and studied it as an alternative approach to obtain a broadband emission centered at ~1 μm with high emission intensity.

2. Experimental methods

$In_xGa_{1-x}As$ layers were grown on a Si-doped n^+-GaAs (001) substrate using molecular beam epitaxy. Figure 1(a) shows a schematic illustration of the grown sample. A GaAs buffer layer with a thickness of approximately 300 nm was first grown on the substrate after a thermal cleaning by heating the substrate at above 600°C for approximately three minutes. Then, an $In_xGa_{1-x}As$ layer embedded between GaAs/$Al_{0.3}Ga_{0.7}As$ layers was grown. Additionally, an $In_xGa_{1-x}As$ layer was grown on the top surface using growth conditions identical to those of the embedded $In_xGa_{1-x}As$ layer to observe its morphology. In order to investigate the dependence of optical and structural properties of the $In_xGa_{1-x}As$ layer on the growth conditions, the growth temperature (T_G) was varied from approximately 420 to 540 °C and the In concentration (x) was varied from 0.2 to 0.34, while the thickness of the $In_xGa_{1-x}As$ layer was fixed at 7 nm. The T_G on the sample surface was measured using a pyrometer, and the x value was estimated by the ratio of InAs and GaAs growth rates for the supplied In, Ga, and As fluxes. Referring to the CLT theoretically estimated by the mechanical equilibrium model of Mathews and Blakeslee [18], the $In_xGa_{1-x}As$ layer thickness of 7 nm is close to the CLT for an x of 0.34, as indicated by the solid line in Fig. 1(b).

The grown $In_xGa_{1-x}As$ layers were characterized by atomic force microscopy (AFM) for

the $In_xGa_{1-x}As$ layer on the top surface, and photoluminescence (PL) measurements were performed at room temperature (RT) for the buried $In_xGa_{1-x}As$ layers. A He-Ne (λ = 632.8 nm) excitation laser was employed for the PL measurements, which had a power density of approximately 300 W/cm^2.

3. Results and discussion

Figure 2 summarizes the surface morphology of the grown $In_xGa_{1-x}As$ layers observed by AFM. The AFM images of the $In_xGa_{1-x}As$ layers with an x value of 0.2 exhibited smooth surfaces independent of T_G. The root mean square (RMS) value of the height in the images was 0.1–0.2 nm less than a single monolayer (ML), which indicates the 2D growth of the layer. In contrast, a rough surface morphology appeared in the $In_xGa_{1-x}As$ layers with higher values for x (0.3 and 0.34) and T_G (>480°C), as indicated within the red frame. The roughness can be seen as 3D structures similar to self-assembled quantum dots or quantum dashes [19], for which the RMS value was approximately 2–3 nm, and the density was approximately 1 × 10^{11} to 2 × 10^{10} cm^{-2}. The surface roughness resulting in the 3D structure could arise from the strain due to the lattice mismatching between InGaAs and GaAs, as previously reported [16,17]. The increase in the RMS value and decrease in the density of the 3D structures may be due to the enhancement of the In migration and coalescence on the surface when T_G was increased from 480 to 520°C. The In migration preferably occurred in the [1-10] direction, and the 3D structure could be elongated and connected in this direction, as typically seen in the samples of $In_{0.3}Ga_{0.7}As$ with T_G = 516°C and $In_{0.34}Ga_{0.66}As$ with T_G = 538°C. A further increase in T_G above 520°C led to the desorption of the supplied In atoms [20], which might have decreased the In concentration. This could be the reason for the surface morphology of the sample of $In_{0.3}Ga_{0.7}As$ with T_G = 536°C.

Figure 3 presents the PL spectra obtained from the grown samples. As shown in Fig. 3(a),

the $In_{0.2}Ga_{0.8}As$ layers exhibited narrow PL lines (a full width at half maximum (FWHM) of approximately 20 meV) in accordance with the 2D (QW) growth observed in the AFM images, while the peak wavelength was gradually blue-shifted from 0.98 to 0.92 μm with the increased T_G. This blue-shift indicates that the In desorption occurred with the T_G increase, and the actual In concentration in the InGaAs layer was decreased from the expected value. As shown in Fig. 3(b), the $In_{0.3}Ga_{0.7}As$ samples exhibited narrow and broad PL spectra, which corresponded to the 2D and 3D structures observed in the AFM images, respectively. The FWHM of the PL peak increased up to approximately 90 meV (T_G = 516°C). The peak wavelength was continuously blue-shifted from 1.05 to 0.94 μm with the increased T_G, which may also have been due to the In desorption. In the case of the $In_{0.34}Ga_{0.66}As$ samples, broadband PL spectra were also seen in the 3D growth structures. However, the peak wavelength was once red-shifted from approximately 1.1 μm at T_G = 437°C to 1.17 μm at T_G = 489°C, and then blue-shifted up to 1.03 μm at T_G = 538°C. The variation of the peak wavelength and FWHM are summarized in Figs. 4(a) and 4(b), respectively. It is still unclear why the red-shift occurred at T_G = 437°C for $In_{0.34}Ga_{0.66}As$, but, it can be speculated that local In segregation occurred and yielded a high In concentrated 3D structure that emitted at the longer wavelength, which resulted from the narrow bandgap of InAs. This behavior might have been influenced by the higher strain with higher In concentration, in contrast to the $In_{0.2}Ga_{0.8}As$ and $In_{0.3}Ga_{0.7}As$ layers. The In segregation might be diluted with the T_G increase, where the In atoms can be migrated on the surface and evaporated, and the peak wavelength could be then blue-shifted.

Regarding the PL intensity, the $In_{0.2}Ga_{0.8}As$ and $In_{0.3}Ga_{0.7}As$ samples exhibited higher peak intensities than the $In_{0.34}Ga_{0.66}As$ samples at T_G values of less than 520°C. However, the peak intensity of an $In_{0.34}Ga_{0.66}As$ sample drastically increased at a T_G above 520°C and was comparable to those of the $In_{0.2}Ga_{0.8}As$ and $In_{0.3}Ga_{0.7}As$ samples, as shown in Fig. 4(c).

Finally, the $In_{0.34}Ga_{0.66}As$ sample at a T_G = 538°C achieved a broadband emission (FWHM of 80 nm) centered at ~1 μm, with a high intensity comparable to that of a normal InGaAs QW. Although the mechanism for the optical properties should be further investigated, it can be attributed to further In migration and desorption resulting in the generation of In(Ga)As 3D nanostructures with large size and In composition distributions, along with a reduction of lattice defects, allowing such a high intensity and broadband emission to be exhibited.

In order to evaluate the broadened emission spectrum from the $In_{0.34}Ga_{0.66}As$ sample at T_G = 538°C for an OCT light source application, a point-spread-function (PSF) was calculated. Figure 5(b) shows the PSF obtained from the PL spectrum (Fig. 5(a)). The PSF was deduced from the autocorrelation, which can be calculated through an inverse Fourier-transformed (IFT) PL spectrum [21]. The PSF governs the axial resolution of the OCT image, and this axial resolution can be estimated using the FWHM of the IFT PL (power) spectra. As shown in Fig. 5(b), the FWHM was approximately 5.7 μm, which is less than that of a typical commercial OCT (~10 μm). In addition, no apparent side lobes appeared beside the main peak. This indicates that the ghost images (noise) resulting from the side lobe should be minimized in an OCT image. These results thus demonstrate the potential of the broadened spectrum for OCT light source application.

4. Conclusion

InGaAs 3D quantum structures were grown on GaAs for a broadband light source that emitted at a wavelength of ~1 μm. By optimizing the growth conditions, including the In concentration, growth temperature, and layer thickness, a broadband and high-intensity emission centered at a wavelength of ~1 μm was obtained. This unique structure offers an alternative method for fabricating a NIR broadband light source that is especially suitable for use as an OCT light source.

Acknowledgements

This study was partly supported by the Grants-in-Aid for Scientific Research (KAKENHI) Grant numbers 25286052 and 16H03858, and by The Terumo Foundation for Life Sciences and Arts.

References

[1] D. Huang, E. A. Swanson, C. P. Lin, J. S. Schuman, W. G. Stinson, W. Chang, M. R. Hee, T. Flotte, K. Gregory, C. A. Puliafito, and J. G. Fujimoto, Science 254 (1991) 1178.

[2] M. E. Brezinski, Optical Coherence Tomography: Principles and Applications, Academic Press, 2006.

[3] M. S. Patterson, B. C. Wilson, D. R. Wyman, Lasers in Medical Science 6 (1991) 379.

[4] N. Ozaki, D. T. D. Childs, J. Sarma, T. S. Roberts, T. Yasuda, H. Shibata, H. Ohsato, E. Watanabe, N. Ikeda, Y. Sugimoto, and R. A. Hogg, J. Appl. Phys. 119 (2016) 083107.

[5] N. Ozaki, T. Yasuda, S. Ohkouchi, E. Watanabe, N. Ikeda, Y. Sugimoto, and R. Hogg, Jpn. J. Appl. Phys. 53 (2014) 04EG10.

[6] N. Ozaki, K. Takeuchi, Y. Hino, Y. Nakatani, T. Yasuda, S. Ohkouchi, E. Watanabe, H. Ohsato, N. Ikeda, Y. Sugimoto, E. Clarke, and R. A. Hogg, Nanomat. Nanotechnol. 4 (2014) 26.

[7] N. Ozaki, K. Takeuchi, S. Ohkouchi, N. Ikeda, Y. Sugimoto, H. Oda, K. Asakawa, and R. A. Hogg, Appl. Phys. Lett. 103 (2013) 051121.

[8] N. Ozaki, K. Takeuchi, S. Ohkouchi, N. Ikeda, Y. Sugimoto, K. Asakawa, R. A. Hogg, J. Cryst. Growth 323 (2011) 191.

[9] P. D. L. Greenwood, D. T. D. Childs, K. M. Groom, B. J. Stevens, M. Hopkinson, and R. A. Hogg, IEEE J. Sel. Top. Quantum Electron. **15**, 757 (2009).

[10] S. K. Ray, K. M. Groom, M. D. Beattie, H. Y. Liu, M. Hopkinson, and R. A. Hogg, IEEE Photonics Technol. Lett. **18**, 58 (2006).

[11] L. Goldstein, F. Glas, J. Y. Marzin, M. N. Charasse, G. Le Roux, Appl. Phys. Lett. 47 (1985) 1099.

[12] Z. Z. Sun, D. Ding, Q. Gong, W. Zhou, B. Xu, Z. G. Wang, Optical Quant. Electron. 31 (1999) 1235.

[13] Z. Y. Zhang, R. A. Hogg, X. Q. Lv, and Z. G. Wang, Adv. Opt. Photon. 2 (2010) 201.

[14] Yuji Hino, Nobuhiko Ozaki, Shunsuke Ohkouchi, Naoki Ikeda, Yoshimasa Sugimoto, J. Cryst. Growth 378 (2013) 501.

[15] Yuma Hayashi, Nobuhiko Ozaki, Shunsuke Ohkouchi, Hirotaka Ohsato, Eiichiro Watanabe, Naoki Ikeda, Yoshimasa Sugimoto, Proceeding of the 43rd International Symposium on Compound Semiconductor (ISCS2016), MoP-ISCS-037.

[16] Shu-Min Wang, Thorwald G. Andersson, Vladimir D. Kulakovskii, and Ji-Yong Yao, Superlattices and Microstructures 9 (1991) 123.

[17] M. J. Ekenstedt, S. M. Wang, and T. G. Andersson, Appl. Phys. Lett. 58 (1991) 854.

[18] J. W. Matthew and A. E. Blakeslee, J. Cryst. Growth 27 (1974) 118.

[19] T. Utzmeier, P. A. Postigo, J. Tamayo, R. Garcia, and F. Briones, Appl. Phys. Lett. 69 (1996) 2674.

[20] S. Chika, H. Kato, M. Nakayama, and N. Sano, Jap. J. Appl. Phys. 25 (1986) 1441.

[21] L. Cohen, IEEE Signal Proc. Lett. 5 (1998) 292.

Figure captions

Fig. 1 (a) Schematic illustration of profile of grown sample. (b) Relationship between the theoretical calculated critical layer thickness (solid line) and the thicknesses of samples grown with various In concentrations (closed circles).

Fig. 2 Summary of AFM images (1×1 μm^2) and RMS values of $In_xGa_{1-x}As$ layers grown with various values for x and T_G.

Fig. 3 PL spectra obtained from $In_xGa_{1-x}As$ layers where $x = 0.2$ (a), 0.3 (b), and 0.34 (c) grown with various T_G values.

Fig. 4 Plots of (a) PL peak wavelength, (b) FWHM, and (c) PL peak intensity as a function of T_G for various values of x.

Fig. 5 (a) PL spectrum obtained from $In_{0.34}Ga_{0.66}As$ layer grown with T_G of 538°C. (b) PSF deduced from the spectrum shown in (a). The FWHM of the PSF, which is approximately 5.7 μm, corresponds to the expected axial resolution of the OCT image.

(a)

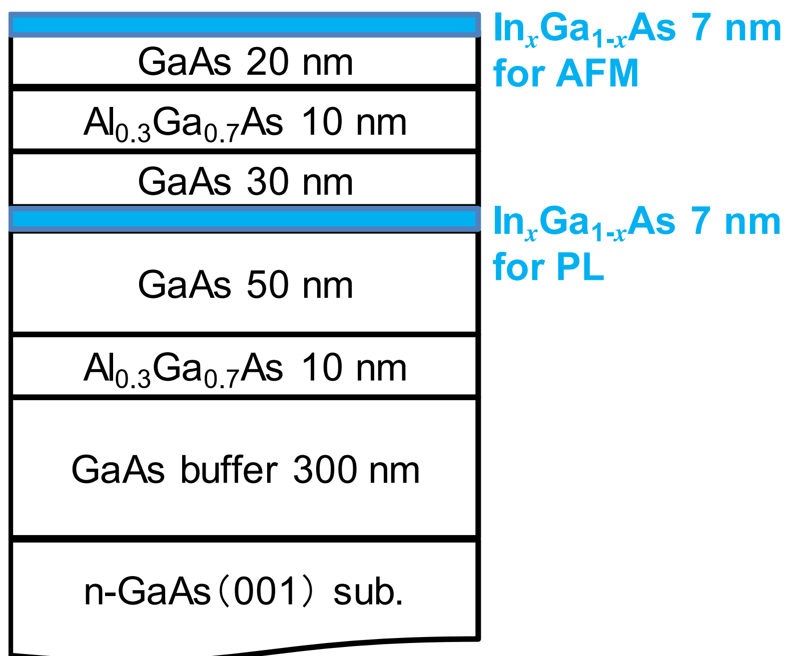

(b)

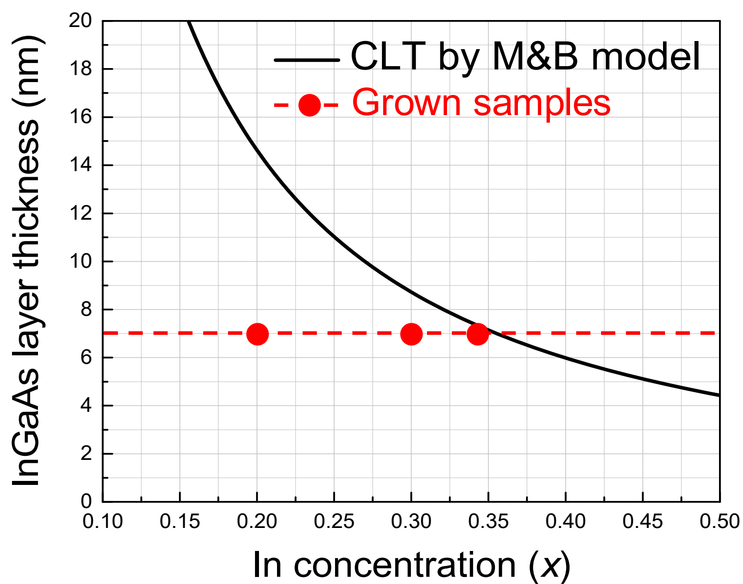

Fig. 1 N. Ozaki et al.

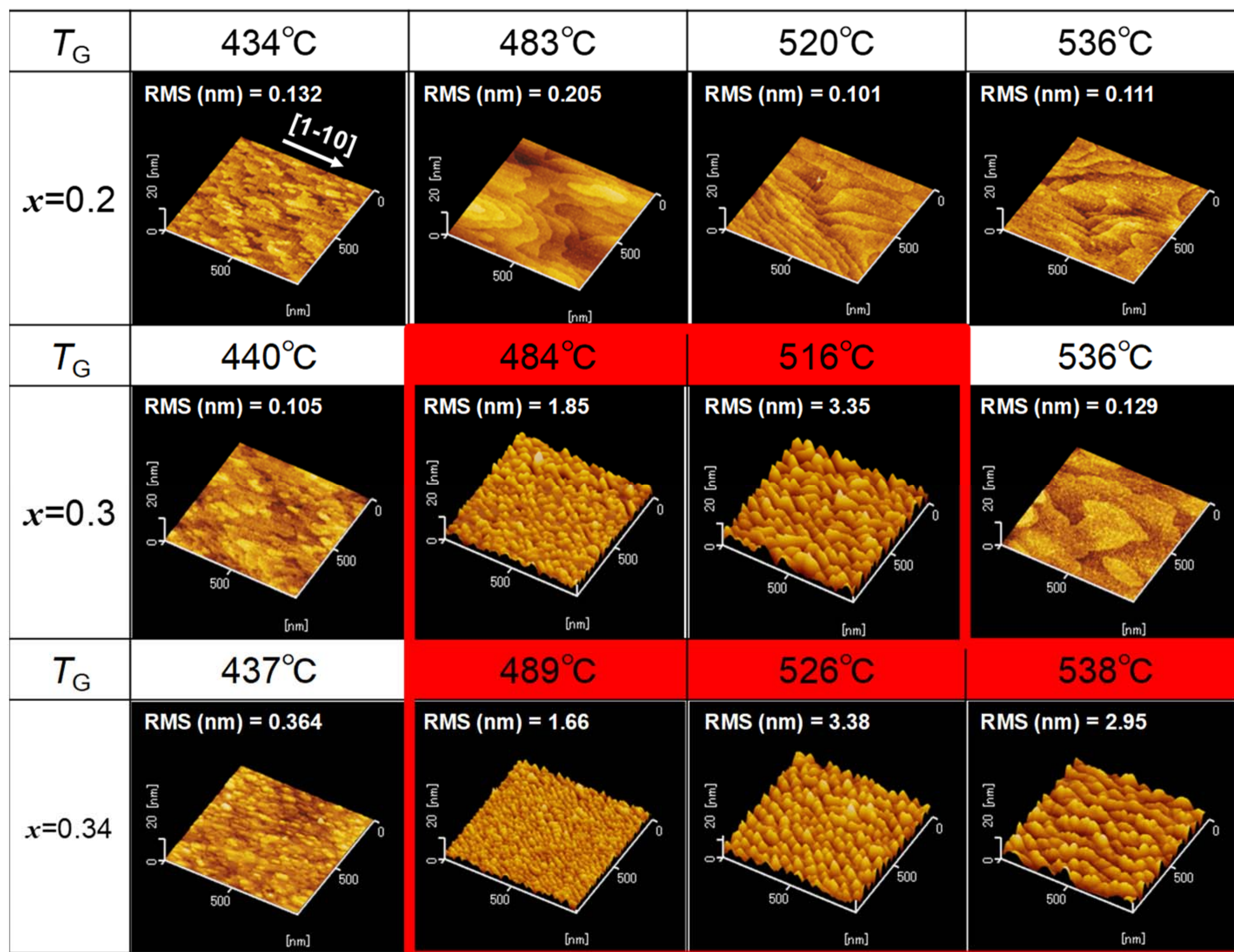

Fig. 2 N. Ozaki et al.

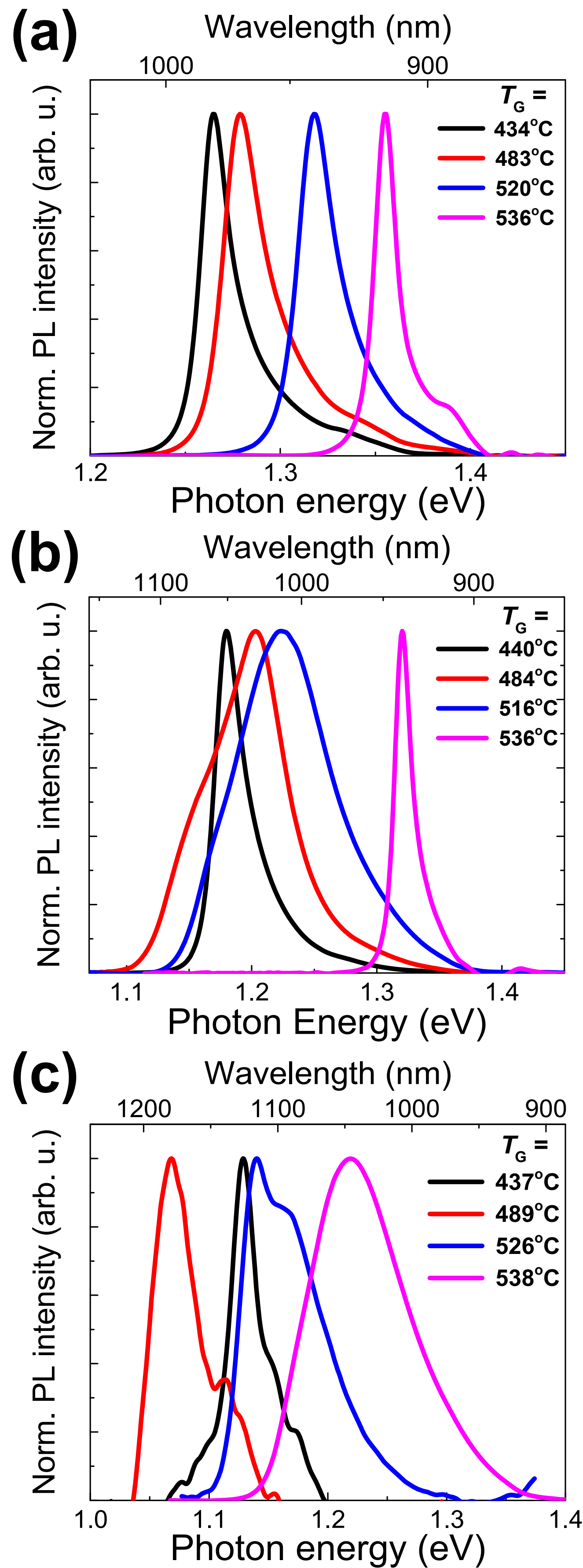

Fig. 3 N. Ozaki et al.

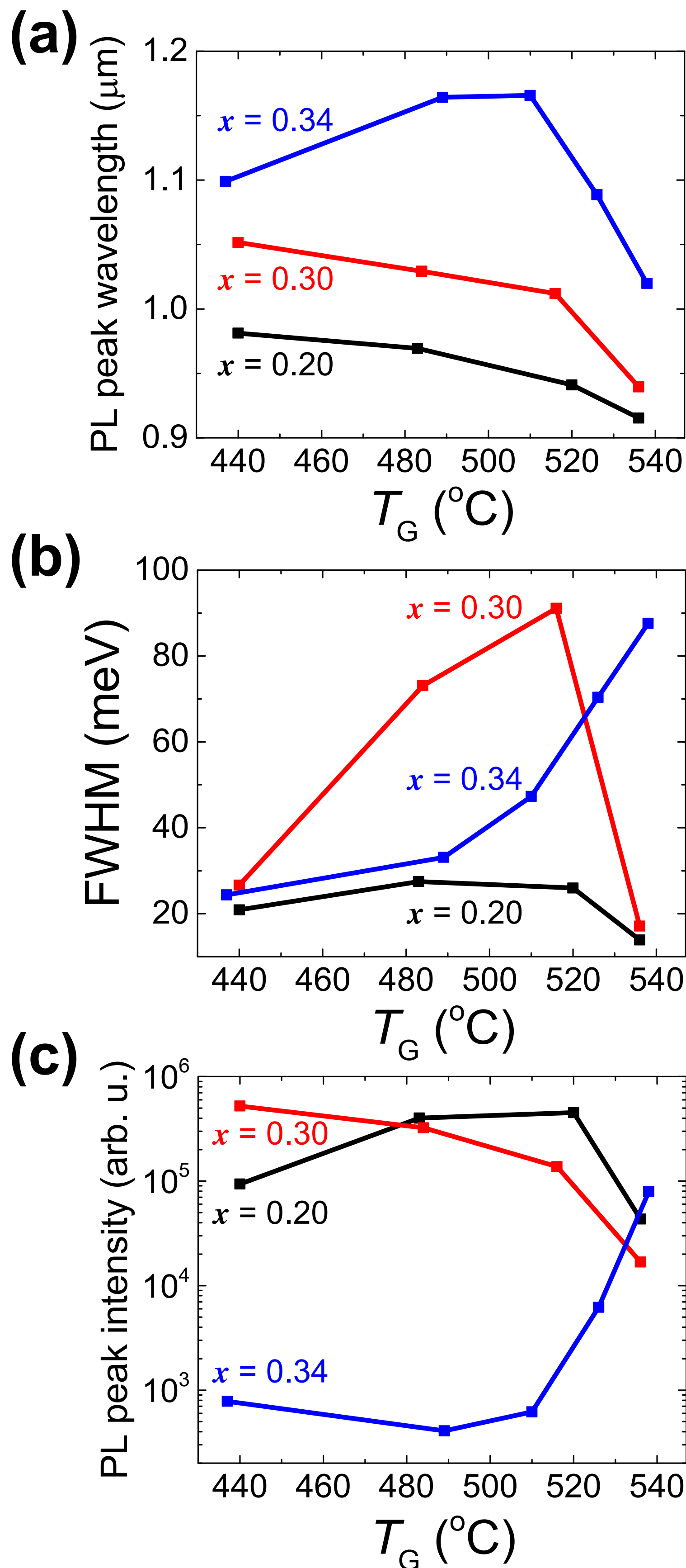

Fig. 4 N. Ozaki et al.

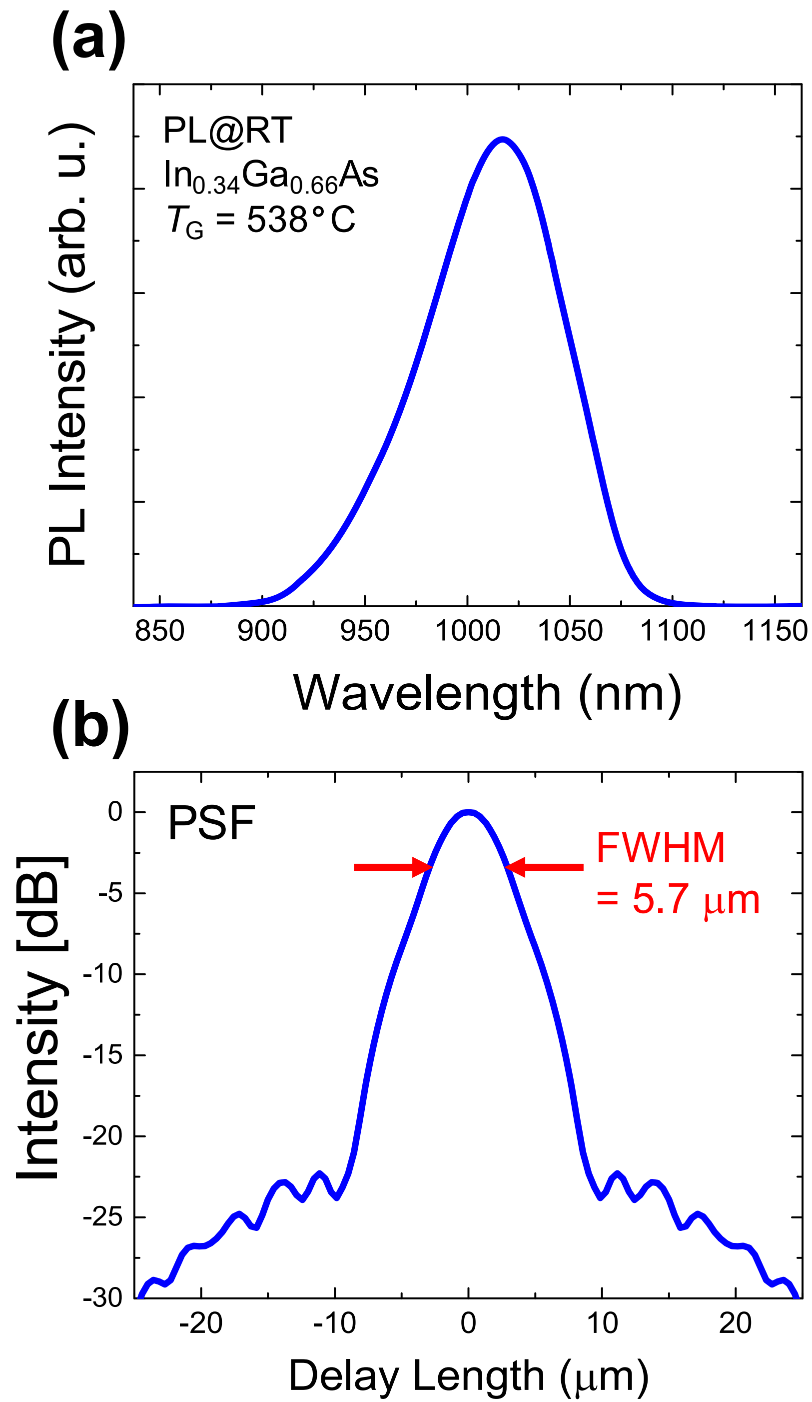

Fig. 5 N. Ozaki et al.